

---

*This copy is for your personal, non-commercial use only.*

---

**If you wish to distribute this article to others**, you can order high-quality copies for your colleagues, clients, or customers by [clicking here](#).

**Permission to republish or repurpose articles or portions of articles** can be obtained by following the guidelines [here](#).

**The following resources related to this article are available online at [www.sciencemag.org](http://www.sciencemag.org) (this information is current as of August 29, 2014 ):**

**Updated information and services**, including high-resolution figures, can be found in the online version of this article at:

<http://www.sciencemag.org/content/280/5369/1596.full.html>

This article **cites 15 articles**, 6 of which can be accessed free:

<http://www.sciencemag.org/content/280/5369/1596.full.html#ref-list-1>

This article has been **cited by** 386 article(s) on the ISI Web of Science

This article has been **cited by** 100 articles hosted by HighWire Press; see:

<http://www.sciencemag.org/content/280/5369/1596.full.html#related-urls>

This article appears in the following **subject collections**:

Neuroscience

<http://www.sciencemag.org/cgi/collection/neuroscience>

cells were then cultured at 37°C overnight and transferred to fresh plates to eliminate adherent cells.

12. J. A. Grasso, N. C. Chromey, C. F. Moxey, *J. Cell Biol.* **73**, 206 (1977); F. Ramirez *et al.*, *J. Biol. Chem.* **250**, 6054 (1975).
13. T. B. Cambell and T. R. Cech, *RNA* **1**, 598 (1995).
14. The mapping library was generated by PCR amplification of plasmid pT7L-21 (7) with a 5' primer containing a randomized sequence at positions corresponding to the ribozyme's IGS (5'-GGGGG-GATCCTAATACGACTCACTATAGNNNNNAAAAGTTATCAGGCATGCACC) and a 3' primer specific for 3' exon tag sequences present in the pT7L-21 plasmid (5'-AGTAGTCTTACTGCAGGGCCTCTTCGCTATTACG). The resulting cDNA library was in vitro transcribed using T7 RNA polymerase to generate the RNA mapping library.
15. RBC precursors ( $1 \times 10^6$  cells) were resuspended in 200  $\mu$ l of Opti-MEM (Gibco-BRL), and ribozymes (2.5 to 5  $\mu$ g generated by *in vitro* transcription) were transfected into these cells using 20  $\mu$ l of DMRIE-C (Gibco-BRL) in 1 ml of Opti-MEM for 4 hours. Then, DMEM (Gibco-BRL) with 10% fetal calf serum (1 ml) and erythropoietin (2 units/ml) were added to the cells. Total RNA was isolated by using TRI Reagent (Molecular Research Center) containing EDTA (10 mM) 16 to 24 hours after transfection. Transfection of these cells with a reporter RNA demonstrated that 1 to 2% of the erythrocyte precursors take up RNA (17).
16. Ribozyme 3' exon (100 to 500 nM) and substrate RNAs (1 to 5  $\mu$ M or 1  $\mu$ g of cellular RNA) were denatured at 95°C for 1 min in reaction buffer [50 mM Hepes (pH 7.0), 150 mM NaCl, 5 mM MgCl<sub>2</sub>] and then equilibrated at 37°C for 3 min. The substrates were then added to the ribozymes along with guanosine (100  $\mu$ M) to start the reactions, which proceeded at 37°C for 3 hours. For reaction mixtures that contained radiolabeled ribozyme, we removed samples at the times indicated and added them to an equal volume of EDTA (10 mM) to stop the reaction. Reaction products were analyzed on a 4% polyacrylamide gel containing 8 M urea. For RT-PCR analysis, trans-splicing products were reverse transcribed at 37°C for 20 min in the presence of L-argininamide (10 mM) from a primer specific for the 3' exon sequence as described (8, 9). The resulting cDNAs were amplified for 30 cycles (*in vitro* ribozyme reactions) or 30 to 90 cycles (*in vivo* ribozyme reactions) using a 3' exon primer (3'tag primer, 5'-ATGCCTG-CAGGTCGACTC; 3'- $\gamma$ -globin primer, 5'-CCGGAAT-TCCCTTGCTCCTCCTGTGA) (9, 20) and a 5' primer specific for the  $\beta$ -globin mRNA (5'-GGG-GATCCTGTGTTCACTAGCAACC). The amplified products were separated on a 10% acrylamide gel and visualized by ethidium bromide staining.
17. N. Lan, unpublished results.
18. J. T. Jones and B. A. Sullenger, *Nature Biotech.* **15**, 902 (1997).
19. Quantitative-competitive RT-PCR analysis of trans-splicing reaction efficiency was performed by incubating  $\beta^S$ -globin RNA with Rib61-3'eff. The 3' exon attached to Rib61-3'eff contains a priming sequence for a downstream RT-PCR primer called down-1 that is also found on the unreacted  $\beta^S$ -globin transcript. After the distance between the down-1 site and an upstream priming site on  $\beta^S$ -globin is spliced, RNA is reduced from 161 to 111 bp. Unreacted globin substrate RNAs as well as revised  $\beta$ -globin products were coamplified by using a single set of PCR primers to yield different-sized products that were separated on an acrylamide gel, and PhosphorImager analysis was used to quantify the efficiency with which the ribozyme had converted the globin RNA to product in the reaction (18).
20. C. Cavallero *et al.*, *Gene* **12**, 215 (1980).
21. In the reactions with the two longer  $\beta$ -globin substrates ( $\beta^S$ -61A<sub>3</sub> and  $\beta^S$ -FL) more free ribozyme is generated than spliced exons. The spliced products have accumulated to about 25% of the level of the free ribozyme at 60 and 180 min. Moreover, 15% and 28% of the 3' exon originally attached to the ribozyme is present in the trans-spliced product band at 60 and 180 min, respectively. This reduced

accumulation does not appear to result from 3' exon hydrolysis, however, because no free 3' exon is detected (Fig. 4A). Rather, this reduction results from cleavage of the trans-spliced products at other sites in these long RNAs by the free ribozyme generated in the reaction. These shorter cleavage products run off the bottom of the gel (17). We did not observe such miscleavage in the case of the short 13-nt substrate 5'SA<sub>3</sub>, however, because the activity of the free ribozymes appears to be suppressed by the excess of unreacted substrate present in the sample (17). The observation that the longer substrates do not appear to suppress this miscleavage as well as their shorter counterpart suggests that not all the longer RNAs are folded into a conformation that allows for ribozyme binding. In the long run, ribozymes with increased substrate specificity will be developed to solve this miscleavage problem.

22. M. T. Ashcroft and P. Desai, *Lancet* **2**, 784 (1976); D. A. Sears, *Am. J. Med.* **64**, 1021 (1978); M. S. Kramer, Y. Rooks, H. A. Pearson, *N. Engl. J. Med.* **299**, 686 (1978).

23. D. R. Powars *et al.*, *Blood* **63**, 921 (1984); D. L. Rucknagel *et al.*, in *Developmental Control of Globin Gene Expression*, G. Stamatoyannopoulos and A. W. Nienhuis, Eds. (Liss, New York, 1987), pp. 487-496.
24. B. A. Sullenger and T. R. Cech, *Science* **262**, 1566 (1993); E. Bertrand *et al.*, *RNA* **3**, 75 (1997).
25. M. J. Telen, R. M. Searce, B. F. Haynes, *Vox Sang.* **52**, 236 (1987).
26. We thank C. Rusconi, P. Zarrinkar, L. Milich, J. Jones, K. Phillips, M. Barman, R. Kaufman, M. Telen, E. Gilboa, H. Lyerly, and R. Rempel for useful discussions, M. Telen for her generous gift of the E6 antibody, and the nurses in labor and delivery and the medical oncology treatment center for their assistance in collecting blood samples. Supported in part by the Korean Academic Research Fund of the Ministry of Education (S.-W.L.) and by a grant (HL57606) from the National Heart Lung and Blood Institute (B.A.S.).

8 December 1997; accepted 9 April 1998

## The Tetrameric Structure of a Glutamate Receptor Channel

Christian Rosenmund, Yael Stern-Bach, Charles F. Stevens\*

The subunit stoichiometry of several ligand-gated ion channel receptors is still unknown. A counting method was developed to determine the number of subunits in one family of brain glutamate receptors. Successful application of this method in an HEK cell line provides evidence that ionotropic glutamate receptors share a tetrameric structure with the voltage-gated potassium channels. The average conductance of these channels depends on how many subunits are occupied by an agonist.

Voltage-gated potassium channels are tetramers, and nicotinic acetylcholine receptors are pentamers (1). Brain glutamate receptors are often assumed to be pentamers (2) because they, like the acetylcholine receptor, are ligand-gated. We developed a method to count the number of subunits in the brain glutamate receptor. The key observation upon which our counting method is based is that the mean single-channel current depends on how many of a receptor's binding sites have an agonist bound. The number of binding sites can then be counted by observing the distinct electrophysiological states that a receptor passes through as successively more binding sites become occupied. Successful application of this counting method requires solving three problems. First, because our method counts binding sites, the number of binding sites must equal the number of subunits; in addition, the binding sites must be equivalent

so that sites are not missed. We therefore used the  $\alpha$ -amino-3-hydroxy-5-methyl-4-isoxazol propionate (AMPA)-receptor GluR3<sub>flip</sub> (and mutant versions) expressed in a mammalian (HEK) cell line (3), because this receptor forms homomultimers.

Second, at the saturating concentrations of agonist that are needed to ensure full binding-site occupancy, the lifetime of each occupancy state is too brief to resolve. To prolong the lifetime of each state, we slowed down the agonist binding rate by interposing a very slow step, the dissociation of a high-affinity competitive antagonist; thus, we started the receptor with all of its binding sites occupied by a competitive antagonist and then made the sites available for agonist binding, one by one, as the bound antagonist molecules slowly dissociated. We used a rapid superfusion system to change an outside-out patch's environment from a saturating concentration of the high-affinity antagonist 6-nitro-7-sulphamoylbenzo(F)quinoxalinedion (NBQX) to a saturating concentration of agonist (4).

Finally, if the receptor's normal desensitization mechanisms were intact, the receptor would desensitize long before this progression through the various occupancy states is complete (5). We therefore used single channels of a GluR6/GluR3 chimera

C. Rosenmund, Workgroup Cellular Neurobiology, Max-Planck-Institute for Biophysical Chemistry, Göttingen, Germany.

Y. Stern-Bach, The Hebrew University-Hadassah Dental School, Department of Anatomy and Embryology, Post Office Box 12272, Jerusalem, Israel.

C. F. Stevens, Howard Hughes Medical Institute, The Salk Institute, La Jolla, CA 92037, USA.

\*To whom correspondence should be addressed. E-mail: cfs@salk.edu

in which desensitization is completely absent (Fig. 1A) (6).

Our key observation is that the receptor passes through three distinguishable states, each with a different mean conductance, as all binding sites become occupied in turn. The transition into the first of these states occurs with two time constants, whereas each of the two remaining states relax with a single time constant. The most straightforward interpretation of these data is that the receptor is a tetramer.

Our experiment required recording from single channels. Determining if a patch has only a single channel was easy, because we used saturating agonist concentrations (for example, quisqualate, 1 mM) that consistently caused our noninactivating channels to open to an apparent 23 pS state with  $88.3 \pm 5\%$  ( $n = 6$ ) probability (Fig. 1A). The increased probability of an open state that results when channel desensitization is removed has been also reported for native AMPA receptors (7).

Figure 1, B and C, exhibits the basic phenomenon. An outside-out patch containing a single GluR6/GluR3 channel was rapidly switched between saturating concentrations of NBQX (10 to 30  $\mu\text{M}$ ) and agonist quisqualate (1 mM). The channel starts in its closed state C and then progresses "staircase" fashion through three distinguishable conducting states that we call S (small, approximately 5 pS mean conductance), M (medium, 15 pS), and L (large, 23 pS).

The channel proceeds through the same three states in the SML order with each antagonist/agonist switch, but the dwell time in each state varies randomly from one switch to the next. When the agonist is removed or replaced by antagonist, the receptor passes in the reverse LMS order to the closed state (Fig. 1B).

To determine whether these three distinct states are an artifact of the GluR6/GluR3 chimeras used, we did the antagonist/agonist switch on GluR3<sub>flip</sub> homomultimeric receptors treated with 100  $\mu\text{M}$  cyclothiazide to remove inactivation (7, 8). Channels constructed from native subunits reveal the same "staircase" behavior (Fig. 1E;  $n = 4$ ).

How can we know that the rate-limiting step in the "staircase" response is dissociation of antagonist? We used a lower affinity competitive antagonist, 5,7-dinitro-quinoxalinedione (MNQX,  $\text{IC}_{50} = 2.2 \mu\text{M}$ ) instead of NBQX ( $\text{IC}_{50} = 150 \text{ nM}$ ) (9). As expected if the rate-limiting step is antagonist dissociation, the channel progressed through the same states in the SML order when MNQX was substituted for NBQX, but the rate of progression was increased about 30-fold (Fig. 1, C and D;  $n = 5$ ).

If the states we identified do indeed correspond to different numbers of bound agonist molecules, then the current amplitude histogram should change in an orderly way as the agonist concentration is increased. At the lowest agonist concentrations, the S state should predominate; at very high agonist concentrations the channel should be always in the L state, and the amplitude histogram should exhibit a mixture of states in between. This prediction is confirmed by the amplitude histograms shown in Fig. 1G for agonist concentrations of 1 to 300  $\mu\text{M}$  (compare Fig. 1, F and G).

Correct counting of binding sites requires an analysis of dwell times at each step along the "staircase." The distribution of dwell times combined from eight patches is shown (Fig. 2A). The second (S  $\rightarrow$  M) transition is most rapid (mean dwell time =  $224 \pm 9.1 \text{ ms}$ ), the last (M  $\rightarrow$  L) is slowest ( $461 \pm 20.3 \text{ ms}$ ), and the first (C  $\rightarrow$  S) transition is intermediate ( $258 \pm 9.9 \text{ ms}$ ). Note also that the waiting times for the S  $\rightarrow$  M and M  $\rightarrow$  L transitions are exponential, but that the C  $\rightarrow$  S transition exhibits two clear components.

A first guess might be, "Three states,

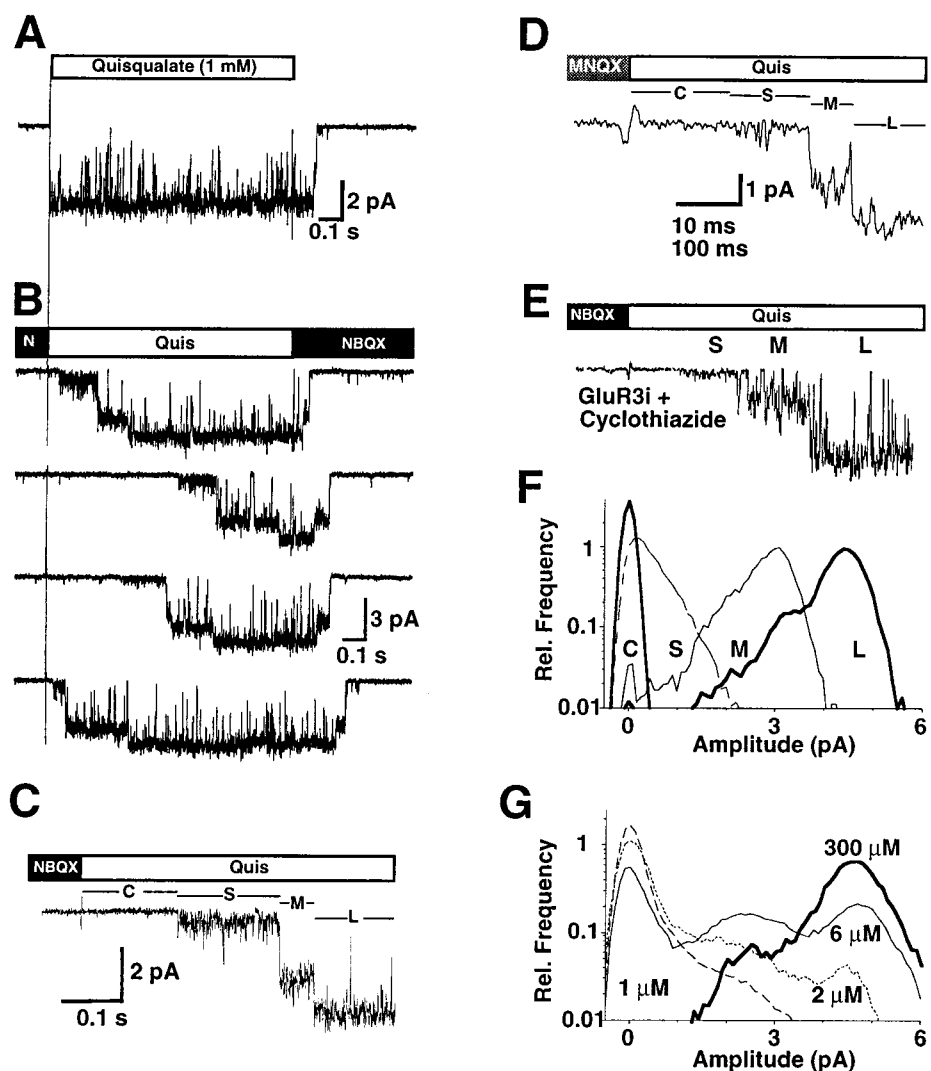


**Fig. 1.** (A) A response from an outside-out patch containing a single AMPA receptor (GluR6/GluR3) during a 1-s concentration step from control solution into quisqualate (1 mM) and back. Holding potential,  $-160 \text{ mV}$ . Filtered at 2 kHz. (B) Four individual responses [different patch from (A)], with step from NBQX (10 to 30  $\mu\text{M}$ ) into quisqualate (1 mM). After some delay, two intermediate (approximately 5 and 15 pS) states preceded the same large conductance seen in (A). Filtered at 1 kHz. Holding potential,  $-160 \text{ mV}$ . (C) The same patch is shown as in (B); Note the time scale. (D) The same patch is shown as in (C), but with a low-affinity competitive antagonist MNQX (300  $\mu\text{M}$ ). Note the different time scale compared to (C). Scale bar: 1 pA and 10 ms. (E) NBQX/quisqualate switch for a single GluR3<sub>flip</sub> channel treated with 100  $\mu\text{M}$  cyclothiazide. The scale bar (1 pA, 100 ms) appears in (D). (F) Amplitude histograms for the states C, S, M, and L averaged from 10 consecutive episodes of antagonist/agonist switches. Same patch as in (B), (C), and (D). (G) Amplitude histograms for a single nondesensitising channel activated with 1, 2, 6, and 300  $\mu\text{M}$  1-quisqualate.

three subunits: it's a trimer." This initial notion is inconsistent with our data, however, because it can explain neither the two-component waiting time distribution for  $C \rightarrow S$  nor the fact that the  $S \rightarrow M$  transition is fastest.

The simplest theory consistent with a two-component waiting time distribution for

the  $C \rightarrow S$  transition and single-component waiting time distributions for the subsequent transitions would have the first ( $C \rightarrow S$ ) transition involve the dissociation of two antagonists (and the binding of two agonists) and to have each of the other transitions require only a single antagonist dissociation. This model implies four subunits

(10). According to this view, occupancy of two binding sites is necessary for channel opening, but each additional occupancy increases mean single-channel current. If binding sites are identical and independent, then this theory makes specific predictions (10) about all of the waiting time distributions (illustrated in Fig. 2, A through C) with only a single free parameter  $\tau$ , the average time an antagonist remains on its binding site. As can be seen from the smooth curves in Fig. 2, A through C, the simple theory provides a satisfactory fit to the data (Kolmogorov-Smirnov test,  $P > 0.2$ ). We examined similar alternative schemes, like three subunits or five subunits with two or three occupancies required for a channel opening, and find that they do not fit the waiting time data satisfactorily (Fig. 2, C and D).

Our model accurately predicts the relative mean dwell times in the various states with no parameters estimated from the data (10). The predicted ratio of the waiting times ( $C \rightarrow S$ )/( $S \rightarrow M$ ) is  $(1/4 + 1/3)/(1/2) = 7/6 = 1.17$ , and the observed ratio for eight patches is  $1.15 \pm 0.07$ . The predicted ratio for the ( $M \rightarrow L$ )/( $S \rightarrow M$ ) waiting times is  $1/(1/2) = 2$ , and the observed ratio (same patches) is  $2.06 \pm 0.13$ .

We conclude that the glutamate receptor we studied is most likely a tetramer. This conclusion is not, perhaps, completely unexpected for several reasons, despite the common assumption that the glutamate receptors are pentamers (2). First, biophysical and biochemical studies on the *N*-methyl-D-aspartate (NMDA)-type glutamate receptor suggest four binding sites, although a pentameric structure has recently been proposed by Premkumar and Auerbach (11). Second, using a biochemical approach, Mano and Teichberg (12) report a tetrameric structure for glutamate receptors. Finally, the glutamate receptor pore structure may be like that of the potassium channel, which is known to be tetrameric (1). Our data support a tetramer, but we cannot, of course, exclude more elaborate schemes with more than four subunits that interact in whatever complicated way necessary to look like four independent subunits.

Perhaps the most interesting observation we made is that the average conductance of this channel, like that of the cyclic nucleotide-gated channel (13), depends on the number of binding sites occupied by agonist molecules. Because agonist binding seems to be required for the channel-opening conformational change, our observation leads to a model in which a single subunit can open the receptor's pore a certain amount and conformational changes in multiple subunits can open it more. Chapman *et al.* proposed a similar picture for delayed rectifier channels drk1 (14). In addition to the

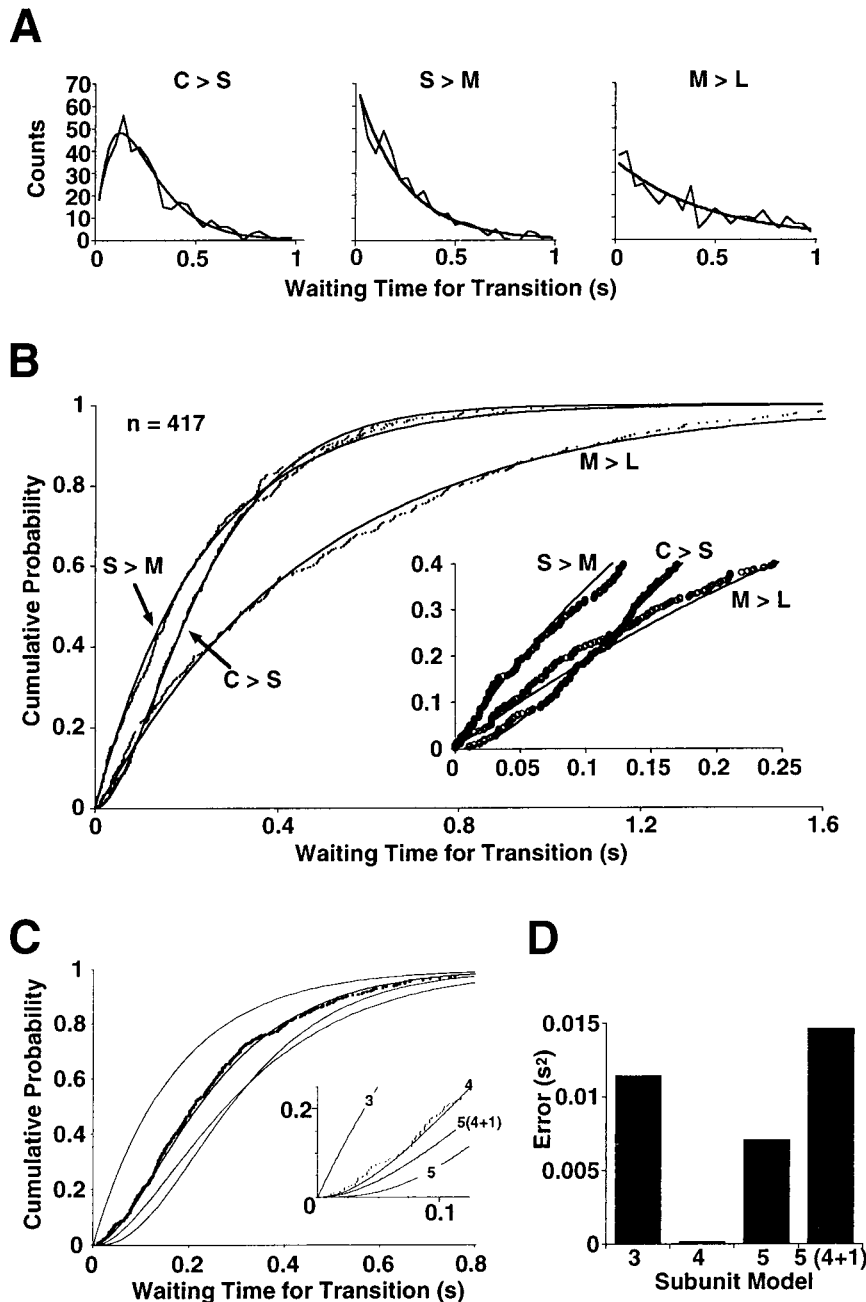


**Fig. 2.** Waiting times reveal four subunits. **(A)** Histogram of waiting times for  $C \rightarrow S$ ,  $S \rightarrow M$  and  $M \rightarrow L$  transitions from 417 episodes (eight patches). Four-subunit theory superimposed (11) with  $\tau = 462$  ms. **(B)** Cumulative probability versus waiting times with predictions from the four-subunit model (11). Same observations and theory as in (A). Inset: expanded data and the same theory. **(C)** Cumulative probability for the  $C \rightarrow S$  waiting time for different models as indicated by numbers associated with expanded graph in inset (11). **(D)** Four-subunit model and alternatives. We calculated the sum of the squared deviations between predicted and observed mean waiting times such that the sum of waiting times adds up to the observed 943 ms (ordinate); the numbers on the abscissa indicate the various models (11).

differences in single-channel conductance based on the subunit composition (15), the notion that conductance levels represent the conformational state of GluRs helps to explain why so many conductance levels are seen in natural single-channel currents at synapses (16).

## REFERENCES AND NOTES

- N. Unwin, *Cell (suppl.)* **72**, 31 (1993); M. W. Wood, H. M. A. VanDongen, A. M. J. VanDongen, *Proc. Natl. Acad. Sci. U.S.A.* **92**, 4882 (1995); R. MacKinnon, *Neuron* **14**, 889 (1995); M. A. Raftery, et al., *Science* **208**, 1454 (1980); A. Karlin, *Curr. Opin. Neurobiol.* **3**, 299 (1993).
- D. Blackstone et al., *J. Neurochem.* **58**, 1118 (1992); R. J. Wenthold, N. Yokotani, K. Doi, K. Wada, *J. Biol. Chem.* **267**, 501 (1992); N. Brose, G. P. Gasic, D. E. Vetter, J. M. Sullivan, S. F. Heinemann, *ibid.* **268**, 22663 (1993); T. Y. Wu and Y. C. Chang, *Biochem. J.* **300**, 365 (1994); M. J. Sutcliffe, Z. G. Wo, R. E. Oswald, *Biophys. J.* **70**, 1575 (1996); A. V. Ferrer-Montiel and M. Montal, *Proc. Natl. Acad. Sci. U.S.A.* **93**, 2741 (1996); I. Mano and V. I. Teichberg, *Soc. Neurosci. Abstr.* **22**, 726 (1996); A. Kuusinen, M. Anvola, K. Keinänen, *EMBO J.* **14**, 6327 (1995).
- M. Hollmann and S. Heinemann, *Annu. Rev. Neurosci.* **17**, 31 (1994).
- After patch excision, we used a rapid perfusion system [C. Rosenmund, A. Feltz, G. L. Westbrook, *J. Neurosci.* **15**, 2788 (1995)] to produce rapid (200 to 400  $\mu$ s) concentration changes at 0.1 to 0.2 Hz. The three-barreled squared capillary was filled with control, agonist, and antagonist. Switches were made from control  $\rightarrow$  agonist  $\rightarrow$  control and antagonist  $\rightarrow$  agonist  $\rightarrow$  antagonist. A version of this rapid switching method has been used previously to count binding sites [J. D. Clements, A. Feltz, Y. Sahara, G. L. Westbrook, *J. Neurosci.* **18**, 119 (1998)]. We tried several agonists (for example, S-AMPA, glutamate), but quisqualate was most commonly used because it dissociated most slowly (half-decay times: AMPA =  $64 \pm 8$  ms,  $n = 5$ ; glutamate  $6.2 \pm 2.6$  ms,  $n = 5$ ; quisqualate =  $106 \pm 21$  ms,  $n = 6$ ). Pipettes were filled with 150 mM CsF, 20 mM HEPES, 2 mM  $MgCl_2$ , 10 mM NaCl, 10 mM EGTA, and were adjusted to 320 mOsm and pH 7.3. The holding potential was  $-60$  to  $-160$  mV, and experiments were at room temperature. Currents were recorded with an Axopatch amplifier 200 B (Axon Instruments, Foster City, CA), low-pass filtered at 1 to 5 kHz, and digitized at 2 to 20 kHz. The extracellular medium contained 170 mM NaCl, 10 mM HEPES, 2 to 4 mM  $CaCl_2$ , 2 to 4 mM  $MgCl_2$ , and was adjusted to 330 mOsm and pH 7.25. Drugs were obtained from Tocris Cookson Ltd. (Bristol, UK) and dissolved in water- or dimethylsulfoxide-based stock solutions. Maximal final dimethylsulfoxide concentration was 0.1%.
- I. Kiskin, O. A. Krishtal, A. Tsyndrenko, *Neurosci. Lett.* **63**, 225 (1986); H. Dudel, C. Franke, H. Hatt, *Biophys. J.* **57**, 533 (1990); C.-M. Tang, M. Dichter, M. Morad, *Science* **243**, 1474 (1989).
- Y. Stern-Bach et al., *Neuron* **13**, 1345 (1994); C. Rosenmund and C. F. Stevens, *Biophys. J.* **70**, A251 (1996).
- A. Yamada and C. M. Tang, *J. Neurosci.* **13**, 3904 (1993).
- M. Partin et al., *Mol. Pharmacol.* **46**, 129 (1994).
- J. C. Watkins, P. Krosggaard-Larsen, T. Honore, *Trends Pharmacol. Sci.* **11**, 25 (1990).
- We assume: The receptor has four identical subunits with independent binding sites. Antagonist dissociation is rate limiting with a time constant  $\tau$ , and the agonist concentrations are saturating. State C corresponds to binding of zero or one agonist; when two agonists are bound, the receptor enters state S; with three agonists bound, state M is entered; and the receptor is in state L when all four of its binding sites are occupied. After the antagonist/agonist switch, the mean waiting time  $t_1$  for the C  $\rightarrow$  S transition would be  $t_1 = (\tau/4 + \tau/3)$ . For the S  $\rightarrow$  M transition, the waiting time  $t_2$  would be  $t_2 = \tau/2$ . Finally, when only a single antagonist remains, the time  $t_3$  for the final M  $\rightarrow$  L transition is just  $t_3 = \tau$ . The total time for all three transitions is  $(\tau/4 + \tau/3 + \tau/2 + \tau) = \tau(1/4 + 1/3 + 1/2 + 1) = 2.083\tau = 943$  ms (measured), so  $\tau$  is estimated to be 453 ms. Note that this is close to the time for the M  $\rightarrow$  L transition ( $461 \pm 20.3$  ms), as predicted. The sum of the squared deviations of the predicted waiting times  $t_i$  from the observed values (measured in seconds) is used in Fig. 2D. This is a Poisson jump processes with probability distributions for waiting times (1: C  $\rightarrow$  S),  $P_1(t) = 1 + 3e^{-4t/\tau} - 4e^{-3t/\tau}$ ; (2: S  $\rightarrow$  M),  $P_2(t) = 1 - e^{-2t/\tau}$ ; and (3: M  $\rightarrow$  L),  $P_3(t) = 1 - e^{-t/\tau}$ , where  $P_i(t)$  is the probability of waiting  $t$  or fewer seconds for the indicated  $i$ th transition and  $\tau$  is the mean time for an antagonist dissociation. We also considered three alternative schemes. (i) Three identical binding sites with a single antagonist dissociation required for a transition. This is model 3. (ii) Five identical binding sites with three dissociations required for the C  $\rightarrow$  S transition. This is model 5. (iii) Five identical binding sites with two dissociations required for the C  $\rightarrow$  S transition and with a silent dissociation for the fifth site (that is, state L occurs if either 0 or 1 antagonists are bound). This is model 5(4 + 1). The mean waiting times for each transition are calculated as above with  $\tau(1/3 + 1/2 + 1) = 943$  ms to give  $\tau = 514$  ms for (i),  $\tau(1/5 + 1/4 + 1/3 + 1/2 + 1) = 943$  ms to give  $\tau = 413$  ms for (ii),  $\tau(1/5 + 1/4 + 1/3 + 1/2) = 943$  ms to give  $\tau = 734$  ms for (iii). Predicted values  $t_i$  for the three mean waiting times are used to quantify the goodness of fit for each model by calculating the sum of the squared deviations of the predicted waiting times from the observed values as was done above; these measures are presented in Fig. 2D. The probability distributions for waiting times predicted by these alternatives are: (i)  $P_1(t) = 1 - e^{-3t/\tau}$ ; (ii)  $P_1(t) = 1 - 6e^{-5t/\tau} + 15e^{-4t/\tau} - 10e^{-3t/\tau}$ ; and (iii)  $P_1(t) = 1 + 4e^{-5t/\tau} - 5e^{-4t/\tau}$ ; these equations are used for the predictions in Fig. 2C with the values of given above.
- M. Benveniste and M. L. Mayer, *Biophys. J.* **59**, 560 (1991); J. D. Clements and G. L. Westbrook, *Neuron* **7**, 605 (1991); B. Laube, H. Hirai, M. Sturgess, H. Betz, J. Kuhse, *ibid.* **18**, 493 (1997); L. S. Premkumar and A. Auerbach, *J. Gen. Physiol.* **110**, 48 (1997).
- I. Mano and V. I. Teichberg, *Neuroreport* **9**, 327 (1998).
- L. Ruiz and J. W. Karpen, *Nature* **389**, 389 (1997); R. Taylor and D. A. Baylor, *J. Physiol. (London)* **483**, 567 (1995).
- L. Chapman, H. M. VanDongen, A. M. VanDongen, *Biophys. J.* **72**, 708 (1997).
- T. Swanson, S. K. Kamboj, S. G. Cull-Candy, *J. Neurosci.* **17**, 58 (1997).
- E. Jahr and C. F. Stevens, *Nature* **325**, 522 (1987); S. G. Cull-Candy and M. M. Usowicz, *ibid.*, p. 525.
- We thank B. Seed for the CD8 vector, Eli Lilly Corp. for the cyclothiazide, and the mechanics department of the Max-Planck-Institute for construction of the fast-flow system. We are indebted to S. Schmidt, S. Russo, the Eli Lilly Corp., G. Swanson, and R. Petroski for their help and advice in the HEK culture and transfection. S. Russo also participated in some of the GluR3 experiments. Supported by a Helmholtz fellowship (C.R.), the Howard Hughes Medical Institute (C.F.S.), and NIH grant NS 12961 (C.F.S.).

8 July 1997; accepted 21 April 1998

## Closing the Circadian Loop: CLOCK-Induced Transcription of Its Own Inhibitors *per* and *tim*

Thomas K. Darlington,\* Karen Wager-Smith,\*  
M. Fernanda Ceriani,\* David Staknis, Nicholas Gekakis,  
Thomas D. L. Steeves, Charles J. Weitz,  
Joseph S. Takahashi, Steve A. Kay†

The circadian oscillator generates a rhythmic output with a period of about 24 hours. Despite extensive studies in several model systems, the biochemical mode of action has not yet been demonstrated for any of its components. Here, the *Drosophila* CLOCK protein was shown to induce transcription of the circadian rhythm genes *period* and *timeless*. dCLOCK functioned as a heterodimer with a *Drosophila* homolog of BMAL1. These proteins acted through an E-box sequence in the *period* promoter. The *timeless* promoter contains an 18-base pair element encompassing an E-box, which was sufficient to confer dCLOCK responsiveness to a reporter gene. PERIOD and TIMELESS proteins blocked dCLOCK's ability to transactivate their promoters via the E-box. Thus, dCLOCK drives expression of *period* and *timeless*, which in turn inhibit dCLOCK's activity and close the circadian loop.

In animals, plants, or prokaryotes, activities such as locomotion or photosynthesis do not occur with equal probability throughout the 24-hour day but are organized by an endogenous circadian oscillator. The oscillator allows the organism to anticipate daily environmental fluctuations rather than merely respond to them. In *Drosophila*, two essential oscillator components, *period* (*per*) and *timeless* (*tim*), have mRNA transcript levels that cycle with a circadian rhythm (1). Mouse homologs of *per* are also

regulated in a circadian fashion (1). Thus, the core mechanism of the circadian oscillator is likely to be conserved between *Drosophila* and mammals.

In *Drosophila*, the *per* and *tim* mRNA oscillations are controlled in large part by transcriptional regulation (2) and some posttranscriptional processes (3). Point mutations in the coding region can change the length of the cycle or abolish it (1), indicating that PER and TIM proteins control their own oscillations. Overexpression of a